Chapter 1

Ultra-Quantum 2D Materials: Graphene, Bilayer Graphene, and Other Hall Systems—New Non-Local Quantum Theory of Hall Physics

Patrycja Łydżba and Janusz Jacak

Additional information is available at the end of the chapter

http://dx.doi.org/10.5772/64018

Abstract

We present a brief introduction of the fractional quantum Hall effect—a description of the phenomenon is provided and basic requirements for its formation are discussed. We recall assumptions of the standard composite fermion theory. Additionally, we present a list of the fractional quantum Hall effect puzzles. The chapter also introduces the non-local approach to quantum Hall physics, which is entirely based on a mathematical concept of braid groups and their reduction stimulated by an external magnetic field (in two-dimensional spaces). We emphasize the connection between a one-dimensional unitary representation of the system braid group and the particle statistics (unavoidable for any correlated Hall-like states). We implement our topological approach to construct hierarchies of FQHE fillings for various two-dimensional structures, including multi-layers. We show the remarkable agreement of our results with experimental findings.

Keywords: the fractional quantum Hall effect, graphene, bilayer graphene, braid groups, topology

1. Introduction to the fractional quantum Hall effect

In high magnetic fields and low temperatures, dips in a longitudinal resistivity ($\rho_{xx} \to 0$) and plateaus in a transverse one ($\rho_{xy} = h/ve^2$) appear for fractional fillings (v) of Landau levels (LLs)—this transport feature is called the fractional quantum Hall effect (FQHE). Mentioned minima show an activated behavior, vanishing exponentially as temperature goes to zero and indicating the presence of a gap in the spectrum [1]. The latter phenomenon, despite its long history

[2], constantly receives a great amount of interest from the scientific society. Though many preliminary requirements for Hall-like states are commonly known, the comprehensive theory of this effect—capable of explaining all experimental findings in an elegant way—is still missing. One of the obvious facts is that the FQHE is impossible to obtain within a single-particle picture without interactions—where a partial filling of an elongated-states band immediately results in a nonzero value of the longitudinal resistivity. Among the explained necessity of strong inter-particle correlations in the system, a two-dimensional (2D) topology and a quantized kinetic energy (flat bands—as in the case of LLs) are also compulsory for evidencing the FQHE. Additionally, due to the fragility of these incompressible states, a high purity of the sample needs to be ensured too.

Let us emphasize that when the lowest Landau level (LLL) is partially occupied (or when a collectivization is restricted to one, arbitrary LL), kinetic energy remains constant ($E_k = \hbar\omega_c$, where $\omega_c = eB/mc$ is a cyclotron angular frequency). This applies also to the background potential energy. The ground state is, thus, expected to minimize the Coulomb repulsion. Since for a wide collection of magnetic fields the FQHE is actually observed, the latter requirement refers to collective Hall-like states (and not Wignier-crystal states with localized electrons [3], as it may seem at first).

The initial step towards an explanation of the FQHE was taken by Laughlin [4], who proposed the exact solution for a basic set of fillings from the LLL, $\nu = 1/q$ (q – odd),

$$\Psi_L = \prod_{i<j}^{N} \left(z_i - z_j\right)^q e^{-\frac{1}{4l_0^2}\sum_{i=1}^{N}|z_i|^2} \tag{1}$$

where N is the number of electrons, $l_0 = \sqrt{\hbar c/eB}$ stands for magnetic length and $z = x + iy$ is a complex position. Note that when two arguments of this wave function are swapped, Ψ_L gains an additional phase equal to $q\pi$. This detail of the solution (or more precisely—the quantum statistics of particles) is usually called the hallmark of Laughlin correlations and included in all theories of the FQHE—as a result of the Aharonov-Bohm effect [5] or the Berry phase acquired by a vortex [6–8]. However, the one-dimensional unitary representations (1DURs) of the full braid group (π_1)—which define the particle statistics—are periodic with a periodicity of 2π ($e^{iq\pi} = e^{i\pi}$ for odd q). In order to deal with this issue, we suggest to associate FQHE particles (so-called composite fermions) with the appropriately constructed braid subgroups of π_1. This allows to differentiate them from ordinary fermions characterized with the full braid group. The latter idea is explained in detail in following sections and in authors' papers [9–11].

Unfortunately, despite its unbelievable accuracy confirmed by exact diagonalization methods (at least for a small amount of particles) [12], the Laughlin wave function was introduced as an ansatz or, if one prefers, as an inspired (educated) guess. Nonetheless, it might be educatory to recall his arguments [4, 13]. First, note that one can choose single-particle eigenstates within LLL (in a central gauge) to be eigenstates of a coordinate of the angular momentum ($\hat{l}_z$),

http://dx.doi.org/10.5772/64018

$$\varphi_m = z^m e^{-\frac{|z|^2}{4l_0^2}} \tag{2}$$

where m (integer) is an eigenvalue of $\hat{l}_z$. It is easy to establish the average area covered by an arbitrary electron, $\langle\varphi_m|\pi r^2|\varphi_m\rangle = 2\pi(m+1)l_0^2$. Thus, the degeneracy of a whole Landau level equals,

$$N_0 = m_{max} + 1 = \frac{S}{2\pi l_0^2} = \frac{SB}{hc/e} \tag{3}$$

where S is a sample surface and $hc/e = \phi_0$ is a magnetic field flux quantum. Additionally, m_{max} stands for a maximal value of m, which produces a state satisfying the $\langle\varphi_m|\pi r^2|\varphi_m\rangle \leq S$ relationship. As a result, the general state of a multi-particle system from the LLL takes the form of,

$$\Psi = f(z_1, z_2, \ldots, z_N) e^{-\frac{1}{4l_0^2}\sum_{i=1}^{N}|z_i|^2} \tag{4}$$

where $f(z_1, z_2, \ldots, z_N)$ is an ordinary polynomial. A degree of this polynomial, D, cannot exceed the maximal $\hat{l}_Z$ eigenvalue realizable in the system. In other words, D is restricted by an inverse of a filling factor times a number of particles (or a degeneracy), $D \leq m_{\max} \approx N_0 = \nu^{-1}N$.

Consider now a two-body problem. The eigenfunction for two particles with a relative angular momentum m and a centre of mass angular momentum M is [13],

$$\varphi_{m,M} = (z_1 - z_2)^m (z_1 + z_2)^M e^{-\frac{1}{4l_0^2}(|z_1|^2 + |z_2|^2)} \tag{5}$$

As long as m and M are assumed non-negative integers, the above state lies entirely in the LLL (it is constructed from linear combinations of one-body functions, φ_m) and, remarkably, appears to be the exact solution of a stationary Schrödinger equation with any central potential acting between two particles. Additionally, eigenvalues of the corresponding Hamiltonian are, simultaneously, eigenvalues of a Coulomb potential, $\hat{V} = \sum_{i<j}^{N} e^2 / |Z_i - Z_j|$ (the fixed kinetic energy can be disregarded—it only adds even shifts to the energy levels),

$$v_m = \frac{\left\langle \varphi_{m,M} | \hat{V} | \varphi_{m,M} \right\rangle}{\left\langle \varphi_{m,M} | \varphi_{m,M} \right\rangle} \tag{6}$$

where v_m expectation values are so-called Haldane pseudopotentials, and they are independent from a central mass angular momentum eigenvalue. Hence, we obtained a discrete spectrum consisted of bound, repulsive potential states. This result is owed to the quenched kinetic energy, and it is possible to obtain only in two-dimensional spaces in the presence of a magnetic field. This finding should not be surprising—the high potential energy of interacting particles cannot be converted into the high kinetic energy (E_k is kept constant within one Landau level) and, hence, particles cannot "fly apart". Even classically, when a third (parallel to the magnetic field) dimension is lacking, the Lorentz force protects electrons from being pushed away from each other.

Let us now return to Laughlin's considerations, concerning the many-body ground-state wave function for filling factors, $v = 1/q$ (q – odd). Though we are currently unable to derive it analytically for $v < 1$, the lowest energy solution for a complete filling of the LLL ($v = 1$) is well known. It can be written as a Slater determinant of all accessible (indexed with an angular momentum eigenvalue) one-particle states [14],

$$\Psi_S = \begin{vmatrix} 1 & z_1 & z_1^2 \dots & z_1^{N-1} \\ \dots & \dots & \dots\dots & \dots \\ 1 & z_N & z_N^2 \dots & z_N^{N-1} \end{vmatrix} e^{-\frac{1}{4l_0^2}\sum_{i=1}^{N}|z_i|^2} = \prod_{i<j}^{N}\left(z_i - z_j\right) e^{-\frac{1}{4l_0^2}\sum_{i=1}^{N}|z_i|^2} \tag{7}$$

where Ψ_S is the Slater function with the Vandermonde polynomial. Taking into account this conclusion, as well as bearing in mind the two-body eigenstate, it seems plausible that $f(z_1, z_2, \dots, z_N)$ have a Jastrow-like form, $\prod_{i<j}^{N}(z_i - z_j)^q$. Another advantage of this choice lies in its tendency to keep electrons apart—there exists a considerable chance that it may reduce the Coulomb repulsion energy. Furthermore, the system is built from electrons, thus, only odd powers in the Jastrow factor are allowed. Finally, when we connect the q – solution with a $v = 1/q$ filling factor (this can supported by the extremal condition $D = m_{\max}$), we arrive at the Laughlin wave function. Generally, it should be emphasized that all presented arguments are insufficient to prove that Ψ_L is a correct, lowest energy eigenfunction of the multi-particle Hamiltonian. However, its excellent compatibility with numerical results [12] entirely justifies a widespread use of the Laughlin ansatz.

Before skipping to another topic it is worth describing two other features of the Laughlin solution. First, the form of this wave function guarantees that every pair of particles has a relative angular momentum greater or equal to q. Thus, it needs to be an exact eigenfunction of the so-called hard-core potential with neglected long range part of the Coulomb repulsion ($v_m^{HC} = v_m$ for $m < q$ and $v_m^{HC} = 0$ for $m \geq q$) [15],

$$\sum_{m=0}^{\infty}\sum_{i<j}^{N} v_m^{HC} P_m(ij)\Psi_L = 0 \tag{8}$$

http://dx.doi.org/10.5772/64018

where the left-hand side equals to the hard-core potential operator (written in terms of projection operators, $P_m(ij)$, that selects states in which particles i and j have relative angular momentum equal to m) times Ψ_L . This implies that a finite amount of energy is needed to excite the system from its (Laughlin) ground state—there exists a gap in the spectrum (Δ). This gap is believed to be stable against perturbations, thus, all corrections arising from differences between the Haldane and the hard-core potential are expected to be small compared to Δ [13].

Finally, one can prove—with the use of a beautiful analogy developed by Laughlin [4]—that the Ψ_L state describes a uniform particle-density. Let us express the probability distribution in terms of the Boltzmann weight, $|\Psi_L|^2 = e^{-H_q} = e^{-(-2q\sum_{i<j}^{N}\ln(z_i-z_j)+\sum_{i=1}^{N}|z_i|^2/2l_0^2)}$ [14]. H_q turns out to be the potential energy of a one-component, two-dimensional classical plasma. Hence, we expect that electrons are distributed uniformly with a density $\rho = 1/(2\pi l_0^2 m)$ in a state described by $1/q$ filling of the LLL.

At this stage, readers should be warned that many incompressible Hall states—connected with filling factors falling out of the basic set ($1/q$ with odd q)—have already been discovered. Inspired by these results, scientists have been searching for the thorough and microscopic theory of the FQHE ever since. We are not going to present all models or ideas introduced by researchers over the years—this is not the aim of this paper. However, before proceeding to the topological explanation, it is worth becoming acquainted (at least briefly) with today's most widely accepted theory—he theory of composite fermions (CFs). In this very short description, we are going to focus on substantial advantages, as well as built-in problems of the approach.

In the CF model [16, 17], it is assumed that the FQHE and the IQHE (integer effect) are deeply connected and can be unified. The latter phenomenon, however, is usually identified with non-interacting particles, while strong correlations are necessary for the appearance of a fractional one. Nonetheless, the mapping can still be obtained if we assume that Coulomb interactions can be utilized—weakly interacting quasi-fermions can appear in the system—for fractional ν (this is, actually, a first tricky part—no one proved that Landau formulation [18] can be used in 2D spaces, where the spectrum of a Coulomb potential energy is discrete). Now, we only need these novel particles to play the same role for the FQHE as electrons for the IQHE.

Jain, who proposed this approach, postulated that quasi-particles are appearing as complexes of electrons with an even number of magnetic field flux quanta (currently identified with vortices [17], though this disambiguation is not entirely clear and might be misleading) and called them "composite fermions". Note that the many-body wave function embraces an additional Aharonov-Bohm phase, $\frac{e}{\hbar c}\oint Adl = \frac{e}{\hbar c}\int Bds = \frac{e}{\hbar c}\phi_0 = 2\pi$, when an electron (as an argument of Ψ_N) is encircling a single quantum [5]. The latter affects the quantum statistics of CFs—when two quasi-particles are exchanging, the wave function acquires a phase factor,

$$e^{i\alpha} = e^{i\pi}e^{i(p-1)\pi} \tag{9}$$

where the first term corresponds to the statistics of ordinary fermions, while the second term —to the half of an Aharonov-Bohm phase for $p-1$ flux quanta pinned to each electron (p is an odd number). We have already mentioned that this is usually presented as an explanation of the Laughlin correlations.

To understand how the assertion of ϕ_0 results in the unification of IQHE and FQHE, it is useful to first consider non-interacting electrons in a completely filled Landau level, $\nu^*=n$ (with integer n). In this case an incompressible state is produced, thus, particles experience the integer (Hall) phenomenon. Furthermore, the evidenced magnetic field, $|B^*|=\phi_0 N/(S\nu^*)$, can be either positive or negative.

Now attach to every electron (e.g. by asserting an infinitely thin, massless solenoid) an even number of flux quanta pointing in +z direction. This converts electrons into composite fermions. Since these quasi-particles witness an unchanged magnetic field (B^*), we may expect them to also experience the IQHE (despite a different general structure of the energy spectrum compared to ordinary fermions). Finally, we have transformed an incompressible state of electrons into an incompressible state of CFs.

In the last step we adiabatically spread flux quanta pinned to electrons, until they become a part of the external magnetic field with an enhanced (or diminished) strength,

$$B=(p-1)\frac{\phi_0 N}{S}\pm\frac{1}{\nu^*}\frac{\phi_0 N}{S} \tag{10}$$

connected with a fractional filling factor of the form (the obtained hierarchy contains all fillings from the basic set – $n=1$ and $p=q$ – but it includes many other ratios too),

$$\nu=\frac{1}{(p-1)\pm\frac{1}{\nu^*}}=\frac{n}{n(p-1)\pm\mathbf{1}} \tag{11}$$

The implemented assumption that a uniform magnetic field can be obtained from detaching localized ϕ_0 was justified—in the original paper [16]—by the uniform density of an initial (IQHE) state. Note that the minus sign in the above equation arises from the possibility of a negative initial field, B^*. Since $(p-1)>\frac{1}{\nu^*}=\frac{\mathbf{1}}{\boldsymbol{n}}$, the resulting B-field is always positive and points in a + z direction. Eventually, we have successfully connected the FQHE of electrons (ν) with the IQHE of composite fermions ($\nu^*=n$)—if and only if we assume that, during this smearing process, only quantitative changes occur in the energy spectrum. Thus, one can say that electrons effectively absorbed $p-1$ flux quanta from the external magnetic field to transform into CFs, which evidence lower magnetic field and form integer quantum Hall state.

Popularity of the CF theory is owed to the fact that it is able to explain most of (experimentally observable) fractions from the LLL. It also gives a prescription for constructing ground-state

http://dx.doi.org/10.5772/64018

(as well as excited-state) wave functions within the lowest Landau band. However, scientists have already stumbled upon a difficulty—the pyramids of fillings from higher levels are not counterparts of the Jain's hierarchy. It is, for example, impossible to justify the appearance of Hall plateaus in the vicinity of $\nu = 5/2$ and 7/2. To deal with this problem, residual interactions between composite particles were introduced to the considerations and they were supposed to turn some of them into higher order composite fermions with different Landau levels. This approach, unfortunately, was rather unsuccessful but, due to the lack of a better explanation, it is still (quite) widely used [19–21].

Moreover, recent experiments on graphene bilayers confirmed that this quasi-particle approach, regardless of its undeniable advantages, cannot embrace the entire physics behind the FQHE [22–24]. This is due to the fact that the most robust plateau in a transverse resistance—in samples consisted of two weakly coupled sheets of atoms—develops near a half filling (and not a one-third filling, as expected from the CF). Additionally, the improvement of sample quality led to the discovery of novel incompressible states that fall out of the Jain's pyramid of fillings, even in the lowest Landau level of standard GaAs/AlGaAs structures. Among them, there are filling factors with odd denominators (like 4/11) and with even denominators (like 3/8).

As a result of the hunt for a model which can find a solution for all mentioned problems, the topological approach to quantum Hall effects was formulated [9]. In this chapter, we briefly recall its basic assumptions and we demonstrate that it provides a topological explanation of Jain's approach (Section 2). Additionally, we demonstrate that it can be used to explain all incompressible Hall-like states observed in conventional 2DEG, monolayer, and bilayer graphene samples (Section 3). We compare our predictions with experimental findings (Section 4).

2. Non-local theory of Hall systems: the origin and generalization of composite fermions

The non-local theory of Hall systems is entirely based on the well-known mathematical concept of braid groups [25]. The full braid group, $\pi_1(\Omega)$, is a homotopy group of an N-particle system configuration space [26],

$$\Omega = \left(M^N \setminus \Delta\right) / S_N \tag{12}$$

where M is a manifold on which particles are placed, S_N stands for the permutation group of N elements (its appearance results from the assumed indistinguishability of carriers) and Δ removes points (creates topological defects) for which positions of at least two classical particles, as M^N coordinates, are the same. Hence, it is consisted of closed trajectories—though the quotient group structure allows initial and final orderings of particles to differ by a permutation—performed in Ω and organized in homotopy classes. In the case of simply

connected manifold, $\pi_1(\Omega)$ is generated by σ_i elements which describe simple exchanges of i'th and $(i+1)$'th carriers (classical—as M^N coordinates). It is worth emphasizing that *quantum particles do not travel braid trajectories*. However, a relationship between topological properties (reflected in a braid group form) with quantum properties of an arbitrary system cannot be ignored. Note that in the standard quantization method, multi-particle state vectors, Ψ_N, are selected as functions from Ω into complex numbers [26]. Thus, when arguments of Ψ_N are encircling a closed path in their configuration space, the multi-particle wave function gains a phase equal to a one-dimensional unitary representation (1DUR) of the corresponding braid from $\pi_1(\Omega)$. Additionally, in the Feynman path integral formulation of the propagator [27], an additional summation over classes of homotopical trajectories needs to be implemented for multiply connected Ω (one measure, $d\lambda$, in a whole path space cannot be defined). The weight factors emerging in this summation are defined by a one-dimensional unitary representation of $\pi_1(\Omega)$. Finally, the braid group shape and its 1DUR determine a quantum statistics of particles in the system (the allowed types of particles are settled by the topology of a manifold and by certain external factors—e.g. anyons may exist only in 2D spaces).

Let us now move back to Hall systems. It seems reasonable to assume that in the presence of a strong magnetic field, trajectories representing elements of the system braid group are of cyclotron orbit type—although, in general, they are not ordinary circles for highly interacting particles. In the topological approach, we define the surface of an LLL cyclotron orbit (as a representative of a braid from $\pi_1(\Omega)$ by the archetype of a correlated incompressible state—the IQHE state. Hence, a plaque which encircles an area equal to $\frac{S}{N_0}=\frac{\phi_0}{B}=\frac{hc}{eB}$ and embraces exactly one flux quantum can be identified with a cyclotron path in the lowest Landau band. In great magnetic fields (as for partial fillings of the LLL), this enclosed surface may be too small to allow an arbitrary particle (as an argument of Ψ_N or M^N coordinate) to reach its nearest neighbor—the Coulomb repulsion protects a uniform distribution. In this situation *simple exchanges, σ_i, are unenforceable and should be excluded from the braid group describing the system*. Note that it may be impossible to organize a $\pi_1(\Omega)$-subgroup (which satisfy group axioms) from remaining classes of trajectories. However, we have already established that the FQHE can be evidenced only for correlated many-body states and, thus, it requires a determined statistics of particles (and a determined system braid group). Seeing that this phenomenon is actually observed in transport measurements, the $\pi_1(\Omega)$ reduction needs to result in the emergence of a new group (*a cyclotron subgroup*), at least for selected fillings. Generators b_i of a latter subgroup stand for novel, multi-loop exchanges of carriers (loopless, σ_i, cannot be defined). Finally, each pair—a subgroup of the full braid group and a condition, a magnetic field strength, upon which this subgroup characterizes the multi-particle system—represents (and can be used to identify) a FQHE state in the LLL [28].

As we have already mentioned, cyclotron subgroups are always generated with multi-loop exchanges. Thus, trajectories (circled in M-space) representing b_i elements need to be open—they need to contain an integer number of closed loops, n, and exactly one half-loop. Simultaneously, cyclotron orbits (representatives of braids) are closed by the definition. As a result,

http://dx.doi.org/10.5772/64018

the simplest non-trivial cyclotron paths are generated by b_i^2 elements and, hence, they consist an odd number of loops, $2(n+1/2)=2n+1$. We are going to demonstrate why multi-loop exchanges of particles (as arguments of Ψ_N or M^N coordinates) can be permissible in the system, even when loopless ones are not. For simplicity we restrict (at first) our considerations to $1/q$ (q – odd) fillings of the lowest Landau level. In this case, a single-loop path of a carrier experience q flux quanta per particle in the system and—since an LLL orbit embraces exactly one ϕ_0 – its surface is not large enough to reach a neighboring carrier (σ_i exchanges are unfeasible). In 3D manifolds this also applies to multi-loop trajectories (meaning that effective dimensions of loops are not raised; σ_i exchanges are, however, always accessible because particles can move freely in the direction parallel to the magnetic field)—each loop increases the total surface encircled by the path, as a circumvolution adds a new surface to the coil. Therefore, the latter also increases the magnetic field flux evidenced by the path—an individual loop experience q flux quanta per particle too. In 2D manifolds, however, an additional loop cannot enhance path's area and the evidenced flux remains unchanged (the whole trajectory, which represents an element of the system braid group, experiences q flux quanta per particle). As a consequence, all loops must share the total BS/N per particle quantity, which passes through a single-loop path—each loop receives a diminished portion of BS/N and experiences a lower effective magnetic field, B^*. Additionally, if the number of loops in a trajectory coincides with the inverse of an LLL filling factor, $\nu^{-1}=q$, then every loop evidences exactly one ϕ_0 per particle in the system $(BS/(qN)=BS/N_0=\phi_0)$ and an effective magnetic field defined by the relation,

$$\frac{B^*S}{N}=\frac{1}{q}\frac{BS}{N}\rightarrow B^*=\frac{B}{q} \tag{13}$$

Since on the LLL cyclotron orbit falls a single magnetic field flux quantum, the surface encircled by an arbitrary loop (from the q-loop trajectory) is large enough to reach a neighboring particle (as an argument of Ψ_N or M^N coordinate). *Although the loopless exchanges are not permitted in the system, we have just demonstrated that* $\left(\frac{q-1}{2}\right)$*-loop ones are accessible and they generate the cyclotron subgroup of* $\pi_1(\Omega)$. The explicit form of b_i elements for a $1/q$ filling of the lowest Landau level is presented below,

$$b_i^{(q)}=\sigma_i^q,\quad 1<i<N-1 \tag{14}$$

with 1DURs of the form ($\theta=\pi$ for composite fermions—we stick to this generally confusing name for history reasons),

$$b_i^{(q)}\rightarrow e^{iq\theta},\quad 1<i<N-1 \tag{15}$$

Note that the even-denominator rule (q– odd) follows immediately from the requirement of an open trajectory (as an M-space representative) for b_i. Additionally, Laughlin correlations seem to follow from this cyclotron subgroup formalism, rather than from quasi-particles formulation with auxiliary objects pinned to electrons [10].

Consider now a filling factor, which does not belong to the basic set of fillings ($\nu \neq 1/q$). In this situation, it is impossible for every loop from the q-loop trajectory to embrace exactly one flux quantum attributed to a single particle. We can, however, assume that all $q-1$ loops experience a single ϕ_0 per particle and only last loop evidences a residual (per particle) portion, $\pm\frac{1}{x}\phi_0$. Thus, the total magnetic field flux per particle, BS/N, can be written as follows,

$$\frac{BS}{N} = \frac{1}{\nu}\phi_0 = (q-1)\phi_0 \pm \frac{1}{x}\phi_0 \tag{16}$$

A fortunate situation occurs when x is an integer number. In this case the last loop can embrace an entire flux quantum, as the LLL cyclotron orbit does, when it fits perfectly to the separation of an electron (as an argument of Ψ_N or M^N coordinate) and its arbitrary x'th order neighbor. As a result, *the closing loop (as a representative of a winding of a cyclotron subgroup braid) defines the type of accessible exchanges, which are not consisted of q loopless σ_i (these are not accessible for the system), but are integral exchanges of multi-loop type*. Thus, for filling factors included in the Jain-like hierarchy [16, 17],

$$\nu = \left((q-1) \pm \frac{1}{x}\right)^{-1} \tag{17}$$

a cyclotron subgroup of the full braid group can be defined and it is generated by elements,

$$b_i^{(q)} = \sigma_i^{q-1}\sigma_i\sigma_{i+1}\ldots\sigma_{i+x-1}^{\pm 1}\ldots\sigma_i^{-1}\sigma_{i+1}^{-1} \tag{18}$$

The quantum statistics follows immediately from the 1DUR ($\theta = \pi$ for composite fermions),

$$b_i^{(q)} \to e^{i(q-1\pm 1)\theta}, \quad 1 < i < N-1 \tag{19}$$

In the above considerations, we assumed that the last loop of a q-looped path (as a representative of a trajectory circled in the Ω space) can be overwrapped in a direction opposite to one enforced by the external magnetic field. The latter results in an appearance of the minus sign in Eqs. (16)–(19).

It is reasonable to consider even more complex commensurability conditions (of an area encircled by each loop and a surface attributed to a single particle or a group of x particles)—

http://dx.doi.org/10.5772/64018

where $q-1$ loops, which constitute a simplest non-trivial cyclotron path, are divided into sets characterized by different integer numbers, $a \le b \le c \ldots$ (different evidenced fractions of flux quantum per particle, $\frac{1}{a}\phi_0 \ge \frac{1}{b}\phi_0 \ge \frac{1}{c}\phi_0 \ldots$). These sets need to be of even multitudes, $\alpha \ge \beta \ge \gamma \ldots$, to keep a rational character of the exchange braid,

$$b_i^{(q)} = \left(\sigma_i\sigma_{i+1}\ldots\sigma_{i+a-1}\ldots\sigma_i^{-1}\sigma_{i+1}^{-1}\right)^{\alpha}\cdot\left(\sigma_i\sigma_{i+1}\ldots\sigma_{i+b-1}^{\pm 1}\ldots\sigma_i^{-1}\sigma_{i+1}^{-1}\right)^{\beta}\cdot\ldots \tag{20}$$

q	ν	FQHE	
3	$\frac{1}{2\pm 1/x}$	(−) $\underline{1, \frac{2}{3}, \frac{3}{5}, \frac{4}{7}, \frac{5}{9}}, \frac{6}{11}, \frac{7}{13}, \frac{8}{15}, \frac{9}{17}, \frac{10}{19}, \ldots$	(+) $\underline{\frac{1}{3}, \frac{2}{5}, \frac{3}{7}, \frac{5}{9}, \frac{5}{11}}, \frac{6}{13}, \frac{7}{15}, \frac{8}{17}, \frac{9}{19}, \frac{10}{21}, \ldots$
5	$\frac{1}{4\pm 1/x}$	(−) $\underline{\frac{1}{3}, \frac{2}{7}, \frac{3}{11}, \frac{4}{15}}, \frac{5}{19}, \frac{6}{23}, \ldots$	(+) $\underline{\frac{1}{5}, \frac{2}{9}, \frac{3}{13}}, \frac{4}{17}, \frac{5}{21}, \frac{6}{25}, \ldots$
5	$\frac{1}{2+2\cdot 1/2\pm 1/x}$	(−) $\underline{\frac{2}{5}}, \frac{3}{8}\left(\frac{5}{8}\right), \frac{4}{11}\left(\frac{7}{11}\right), \frac{5}{14}, \frac{6}{17}, \frac{7}{20}, \ldots$	(+) $\underline{\frac{2}{7}}, \frac{3}{10}, \frac{4}{13}\left(\frac{9}{13}\right), \frac{5}{16}, \frac{6}{19}, \frac{7}{22}, \ldots$
5	$\frac{1}{2-2\cdot 1/3\pm 1/x}$	(−) $\underline{1}, \frac{12}{13}, \frac{15}{17}, \frac{6}{7}, \frac{21}{25}, \ldots$	(+) $\underline{\frac{3}{5}}, \frac{12}{19}, \frac{15}{23}, \ldots$
5	$\frac{1}{2-2\cdot 1/4\pm 1/x}$	(−) $\frac{4}{5}, \frac{10}{13}, \frac{3}{4}, \frac{14}{19}\left(\frac{5}{19}\right), \frac{8}{11}, \frac{18}{25}, \ldots$	(+) $\frac{4}{7}, \frac{10}{17}, \underline{\frac{3}{5}}, \frac{14}{23}, \frac{5}{13}\left(\frac{8}{13}\right), \ldots$
5	$\frac{1}{4\cdot 1/2\pm 1/x}$	(−) $\underline{\frac{2}{3}, \frac{3}{5}, \frac{4}{7}, \frac{5}{9}}, \frac{6}{11}, \frac{7}{13}, \frac{8}{15}, \frac{9}{17}, \frac{10}{19}, \ldots$	(+) $\underline{\frac{2}{5}, \frac{3}{7}, \frac{5}{9}, \frac{5}{11}}, \frac{6}{13}, \frac{7}{15}, \frac{8}{17}, \frac{9}{19}, \frac{10}{21}, \ldots$
5	$\frac{1}{2\cdot 1/2+2\cdot 1/3\pm 1/x}$	(−) $\frac{3}{4}, \frac{12}{17}\left(\frac{5}{17}\right), \frac{15}{22}, \ldots$	(+) $\frac{1}{2}, \frac{12}{23}, \ldots$
7	$\frac{1}{6\pm 1/x}$	(−) $\underline{\frac{1}{5}}, \frac{2}{11}, \frac{3}{17}, \frac{4}{23}, \ldots$	(+) $\underline{\frac{1}{7}}, \frac{2}{13}, \frac{3}{19}, \frac{4}{25}, \ldots$
7	$\frac{1}{4+2\cdot 1/2\pm 1/x}$	(−) $\frac{2}{9}, \frac{3}{14}, \frac{4}{19}, \frac{5}{24}, \ldots$	(+) $\underline{\frac{2}{11}}, \frac{3}{16}, \frac{4}{21}, \ldots$

Where q = the number of half loops in the exchange trajectory, ν = the hierarchy of fillings. Plus or minus signs denote the direction of a last loop in the multi-loop cyclotron path. Selected hole states are indicated in brackets. Experimentally observable ratios are highlighted—blue color for ν possible to explain within the CF model and red color for ν out of the Jain hierarchy. Additionally, filling factors of monolayer graphene Hall states (which develop in transport measurements) are underlined.

Table 1. Filling factors obtained from the non-local theory (typical semiconductor structures).

The elements above generate cyclotron subgroups for filling factors from the generalized hierarchy of the form,

$$\nu = (\alpha / a \pm \beta / b \pm \gamma / c \pm \cdots)^{-1} \tag{21}$$

1DURs of the resulting subgroups can also be easily estimated (the scalar representation of a subgroup can be identified with reduced representation of the full $\pi_1(\Omega)$),

$$b_i^{(q)} \to e^{i(\alpha \pm \beta \pm \gamma \pm \ldots)\theta}, \quad 1 < i < N-1 \tag{22}$$

Note that while constructing cyclotron subgroups of this type, one needs to keep an eye on the complexity of generators—highly structured braids are probably unfavorable and near corresponding fillings the Wigner crystal (and not the FQHE) phases may be in favor [29–31]. Filling factors obtained within the non-local theory of Hall systems are gathered in **Table 1**. Note that among these fillings one can find all famous and mysterious v, like $\frac{3}{8}$, $\frac{4}{11}$, $\frac{4}{13}$ and others (marked with red color), which cannot be predicted within the quasi-particle formulation (at least when unclear residual interactions are not implemented) [19, 32–35]. For this reason, the topological approach presented in this chapter is the first one to justify all incompressible (collective) states from the LLL, which appear in transport measurements [28].

Finally, it is also worth mentioning that the pyramid of fillings, established within the topological approach, is a generalized version of the well-known Jain's hierarchy (obtained when $\alpha = q-1$ and $a=1$ are implemented into Eq. 21). Thus, *two artificial flux quanta pinned to electron only model (in a very convenient way) an additional loop, which evidences exactly one ϕ_0 per particle and appears in the exchange trajectory (representing a generator of the system braid group)*. The great dependability of the CF theory in the LLL regime can be explained by highlighting the simplicity of cyclotron subgroups generators in the case of Jain's hierarchy—as it was already emphasized, highly structured braids (usually encountered for different configurations of loops) are probably unfavorable and may not result in pronounced plateaus in Hall resistivity.

3. IQHE and FQHE in conventional 2DEG, monolayer and bilayer graphene

Before we proceed to the main aim of this section, it is worth discussing differences in the Landau level ladder between conventional 2DEG, monolayer and bilayer graphene samples (as well as their possible consequences). We first note that in both graphene structures, LLs are not distributed equidistantly on the energy axis, which was the case for typical quantum wells [36–39]. However, the latter is not reflected in the topological approach—an area encircled by a single-loop cyclotron orbit (A) is proportional to the bare kinetic energy of electrons (E_k) and not the general energy determined by LLs. Since a crystal field cannot affect the value of E_k, the embraced surface of an orbit (representing a $\pi_1(\Omega)$ element) varies in the same manner for monolayer and bilayer graphene as for conventional 2DEG. Explicitly, A is proportional to $2n+1$ (where n stands for an LL index). At the same time, this dependence carries another consequence—the commensurability conditions from higher LLs are different from those encountered in the lowest band (the single-loop cyclotron orbit for $n \neq 0$ embraces

exactly $(2n + 1)\phi_0$ and not a single quantum as in the LLL case). Thus, we expect that pyramids of fillings for levels indexed by $n \neq 0$ are not counterparts of the well-known Jain's hierarchy, which has already been confirmed in experiments [40–42].

An important property of the Landau level ladder is its degeneracy (as a number of sublevels, rather than a number of one-particle states, in a single level). In typical 2DEG systems, the half-spin (usually marked with $\uparrow$ and $\downarrow$) stands for an exclusive degree of freedom and, thus, all Landau bands are doubly degenerated. In graphene materials, however, the existence of a so-called valley pseudospin (isospin)—due to the presence of identical Dirac cones in two non-equivalent corners of the Brillouin zone (usually marked with K' and K)—results in an additional degeneracy of the energy spectrum. As a result, for an arbitrarily picked range of factors $[\nu_1, \nu_2]$, the corresponding partially filled Landau level in monolayer and bilayer graphene samples is different than in conventional quantum-wells. We have already mentioned that commensurability conditions (and so the hierarchies of fillings) for distinct n are not identical. We may, thus, expect that some incompressible states, which are marked with v and occur in one of these structures, may not be permissible for the other one.

It should be emphasized that a nonzero Berry phase causes the monolayer graphene LLL to be placed exactly in the Dirac point—where the valence band meets the conduction band in a gapless energy spectrum [36, 37]. The lowest Landau level is, thus, equally shared between free electrons and free holes (only two, not four, spin-valley branches accessible for one type of particles). Since it is natural to define the filling factor in terms of an electronic density measured from the charge neutrality point, ν is counted with respect to the bottom of a conduction band (a third sublevel) and not the LLL as in typical semiconductors [36, 37]. Generally, this also applies to bilayer graphene; however, not only the LLL is placed exactly in the Dirac point, but also the first Landau band. Obviously, the latter affects and determines the convenient impact factor definition, as well as the number of spin-valley branches of the 1LL available for free electrons.

Finally, it is easy to notice that the non-local theory of Hall systems predicts identical hierarchies of LLL filling factors for typical semiconductor quantum-wells and monolayer graphene samples [31, 43–50]. The latter applies for both sublevels of the lowest band (also in graphene—we take into account only fillings accessible for free electrons). Additionally, collective Hall-like states from the second (spin or spin-valley) branch are described with similar filling ratios $(\nu_{0,2})$ as those from the first one $(\nu_{0,1})$. The only difference is obvious and lies in a constant shift of all fractions, $\nu_{0,2} = 1 + \nu_{0,1}$. As we have already mentioned, the cyclotron subgroup model can be used to describe the FQHE in higher LLs of these structures too—the recipe for its application has been included in subsection 3.1.

The case of bilayer graphene is absolutely unique. The appearance of an additional sheet of carbon atoms (additional surface) leads to completely different commensurability conditions. This, for example, results in a surprising form of the basic set, where $\nu = 1/2$ corresponds to the most prominent incompressible state. We are going to describe this problem in detail in subsection 3.2.

Single-loop FQHE	Paired IQHE	q	ν	FQHE
$\frac{7}{3}, \frac{8}{3}$	$\frac{5}{2}$	3	$2+\frac{1}{3\cdot(2-1/x)}$	$\frac{7}{3}\left(\frac{8}{3}\right), \frac{20}{9}\left(\frac{25}{9}\right), \frac{11}{5}\left(\frac{14}{5}\right), \ldots$
			$2+\frac{1}{3\cdot(2+1/x)}$	$\frac{19}{9}, \frac{32}{15}, \frac{15}{7}, \ldots$
			$2+\frac{1}{3\cdot(2\cdot 1/2-1/x)}$	$\frac{8}{3}\left(\frac{7}{3}\right), \frac{5}{2}, \frac{22}{9}\left(\frac{23}{9}\right), \frac{29}{12}, \frac{12}{5}\left(\frac{13}{5}\right), \ldots$
			$2+\frac{1}{3\cdot(2\cdot 1/2+1/x)}$	$\frac{20}{9}\left(\frac{25}{9}\right), \frac{9}{4}\left(\frac{11}{4}\right), \frac{34}{15}, \ldots$
			$2+\frac{1}{3\cdot(2\cdot 1/3-1/x)}$	$3, \frac{14}{5}, \frac{19}{7}\left(\frac{16}{7}\right), \frac{8}{3}, \frac{29}{11}, \frac{34}{13}, \frac{13}{5}, \frac{44}{17}, \frac{49}{19}, \frac{18}{7}\left(\frac{17}{7}\right), \frac{59}{23}, \frac{64}{25}, \frac{23}{9}, \frac{74}{29}, \frac{79}{31}, \frac{28}{11}, \frac{89}{35}, \frac{94}{37}, \frac{33}{13}\left(\frac{32}{13}\right), \ldots$
$\frac{10}{3}, \frac{11}{3}$	$\frac{7}{2}$	3	$3+\frac{1}{3\cdot(2-1/x)}$	$\frac{10}{3}\left(\frac{11}{3}\right), \frac{29}{9}, \frac{16}{5}\left(\frac{19}{5}\right), \ldots$
			$3+\frac{1}{3\cdot(2+1/x)}$	$\frac{28}{9}, \frac{47}{15}, \frac{22}{7}, \ldots$
			$3+\frac{1}{3\cdot(2\cdot 1/2-1/x)}$	$\frac{11}{3}\left(\frac{10}{3}\right), \frac{7}{2}, \frac{31}{9}, \frac{41}{12}, \frac{17}{5}\left(\frac{18}{5}\right), \ldots$
			$3+\frac{1}{3\cdot(2\cdot 1/2+1/x)}$	$\frac{29}{9}, \frac{13}{4}\left(\frac{15}{4}\right), \frac{49}{15}, \ldots$
			$3+\frac{1}{3\cdot(2\cdot 1/3-1/x)}$	$4, \frac{19}{5}, \frac{26}{7}, \frac{11}{3}, \frac{40}{11}, \frac{47}{13}, \frac{18}{5}\left(\frac{17}{5}\right), \frac{61}{17}, \frac{68}{19}, \frac{25}{7}, \ldots$

Where q = the number of half loops in the exchange trajectory, ν = the hierarchy of fillings. Plus or minus signs denote the direction of a last loop in the multi-loop cyclotron path. Selected hole states are indicated in brackets. Experimentally observable ratios are highlighted—blue color for ν possible to explain within the CF model and red color for ν out of the Jain hierarchy. Additionally, results for different sublevels are separated by three lines.

Table 2. 1LL filling factors obtained from the non-local theory (typical semiconductor structures).

3.1. Higher Landau levels: graphene and conventional 2DEG

We consider a system subjected to external magnetic field, which leads to the partial filling of an arbitrary Landau band ($n>0$). To simplify further discussions, we introduce an additional parameter, m, that enumerates spin (or spin-valley) branches in each LL. The latter is two-valued ($m \in \{0, 1\}$) in the typical 2DEG case and four-valued ($m \in \{0, 1, 2, 3\}$) in the monolayer graphene case. We remind that the area embraced by a single-loop cyclotron orbit in the whole n'th Landau level equals to $(2n+1)\frac{hc}{eB} = \frac{(2n+1)\phi_0}{B}$ (it takes exactly $(2n+1)$ flux quanta and its surface is considerably enhanced, when compared to the LLL orbit). This change of an encircled area modifies—and allows for the existence of novel—commensurability conditions, all of which are listed below.

http://dx.doi.org/10.5772/64018

Single-loop FQHE	Paired IQHE	q	ν	FQHE
$\mathbf{\frac{7}{3}}, \mathbf{\frac{8}{3}}$	$\frac{5}{2}$	3	$2+\frac{1}{3\cdot(2-1/x)}$	$\mathbf{\frac{7}{3}}\left(\mathbf{\frac{8}{3}}\right), \frac{20}{9}, \frac{11}{5}, \ldots$
			$2+\frac{1}{3\cdot(2+1/x)}$	$\frac{19}{9}, \frac{32}{15}, \frac{15}{7}, \ldots$
			$2+\frac{1}{3\cdot(2\cdot 1/2-1/x)}$	$\mathbf{\frac{8}{3}}\left(\mathbf{\frac{7}{3}}\right), \frac{5}{2}, \mathbf{\frac{22}{9}}\left(\mathbf{\frac{23}{9}}\right), \frac{29}{12}, \mathbf{\frac{12}{5}}\left(\mathbf{\frac{13}{5}}\right), \ldots$
			$2+\frac{1}{3\cdot(2\cdot 1/2+1/x)}$	$\frac{20}{9}, \frac{9}{4}, \frac{34}{15}, \ldots$
			$2+\frac{1}{3\cdot(2\cdot 1/3-1/x)}$	$3, \frac{14}{5}, \frac{19}{7}, \mathbf{\frac{8}{3}}, \frac{29}{11}, \frac{34}{13}, \mathbf{\frac{13}{5}}, \frac{44}{17}, \frac{49}{19}, \mathbf{\frac{18}{7}}\left(\mathbf{\frac{17}{7}}\right), \ldots$
$\mathbf{\frac{10}{3}}, \mathbf{\frac{11}{3}}$	$\frac{7}{2}$	3	$3+\frac{1}{3\cdot(2-1/x)}$	$\mathbf{\frac{10}{3}}\left(\mathbf{\frac{11}{3}}\right), \frac{29}{9}, \frac{16}{5}, \ldots$
			$3+\frac{1}{3\cdot(2+1/x)}$	$\frac{28}{9}, \frac{47}{15}, \frac{22}{7}, \ldots$
			$3+\frac{1}{3\cdot(2\cdot 1/2-1/x)}$	$\mathbf{\frac{11}{3}}\left(\mathbf{\frac{10}{3}}\right), \frac{7}{2}, \frac{31}{9}, \frac{41}{12}, \mathbf{\frac{17}{5}}\left(\mathbf{\frac{18}{5}}\right), \ldots$
			$3+\frac{1}{3\cdot(2\cdot 1/2+1/x)}$	$\frac{29}{9}, \frac{13}{4}, \frac{49}{15}, \ldots$
			$3+\frac{1}{3\cdot(2\cdot 1/3-1/x)}$	$4, \frac{19}{5}, \frac{26}{7}, \mathbf{\frac{11}{3}}, \frac{40}{11}, \frac{47}{13}, \mathbf{\frac{18}{5}}, \frac{61}{17}, \frac{68}{19}, \mathbf{\frac{25}{7}}\left(\mathbf{\frac{31}{7}}\right), \ldots$
$\mathbf{\frac{13}{3}}, \mathbf{\frac{14}{3}}$	$\frac{9}{2}$	3	$4+\frac{1}{3\cdot(2-1/x)}$	$\mathbf{\frac{13}{3}}\left(\mathbf{\frac{14}{3}}\right), \frac{38}{9}, \frac{21}{5}, \ldots$
			$4+\frac{1}{3\cdot(2+1/x)}$	$\frac{37}{9}, \frac{62}{15}, \frac{29}{7}, \ldots$
			$4+\frac{1}{3\cdot(2\cdot 1/2-1/x)}$	$\mathbf{\frac{14}{3}}\left(\mathbf{\frac{13}{3}}\right), \frac{9}{2}, \frac{40}{9}, \frac{53}{12}, \mathbf{\frac{22}{5}}\left(\mathbf{\frac{23}{5}}\right), \ldots$
			$4+\frac{1}{3\cdot(2\cdot 1/2+1/x)}$	$\frac{38}{9}, \frac{17}{4}, \frac{64}{15}, \ldots$
			$4+\frac{1}{3\cdot(2\cdot 1/3-1/x)}$	$5, \frac{24}{5}, \frac{33}{7}, \mathbf{\frac{14}{3}}, \frac{51}{11}, \frac{60}{13}, \mathbf{\frac{23}{5}}, \frac{78}{17}, \frac{87}{19}, \mathbf{\frac{32}{7}}\left(\mathbf{\frac{31}{7}}\right), \ldots$

Where q = the number of half loops in the exchange trajectory, ν = the hierarchy of fillings. Plus or minus signs denote the direction of a last loop in the multi-loop cyclotron path. Selected hole states are indicated in brackets. Experimentally observable ratios are highlighted. Additionally, results for different sublevels (only three, accessible in measurement, are presented) are separated by three lines.

Table 3. 1LL filling factors obtained from the non-local theory (monolayer graphene).

1. We first consider a single-loop path (as a representative of a braid from the appropriate braid group). The simplest situation—in which this trajectory fits perfectly to the separation of two neighboring particles—corresponds to $2n+1$ flux quanta attributed to a single electron from the partially filled level,

$$\begin{cases} \dfrac{N_0}{N-(2n+m)N_0}=2n+1 & for\ conventional \\ \dfrac{N_0}{N-(4n-2+m)N_0}=2n+1 & for\ graphene \end{cases} \tag{23}$$

where a denominator of the left-hand side expression counts the number of electrons lying in the n'th LL (in the bottom expression a "−2" factor needs to be omitted, while investigating n=0). Furthermore, the whole fraction determines the number of ϕ_0 per particle from the highest available level. Simultaneously, the right-hand side is also connected to the number of ϕ_0, however, grasped by the single-loop cyclotron orbit. One can easily determine filling factors, which fulfil the above equation,

$$\begin{cases} \nu=\dfrac{N}{N_0}=2n+m+\dfrac{1}{2n+1} & for\ conventional \\ \nu=\dfrac{N}{N_0}=4n-2+m+\dfrac{1}{2n+1} & for\ graphene \end{cases} \tag{24}$$

If the system is described with these ν, then exchanges of nearest neighbors, σ_i, are accessible and they generate $\pi_1(\Omega)$. Something surprising should already be noticed—the full braid group is coupled to the IQHE only for the zeroth Landau band. For other levels, the corresponding filling is fractional (e.g. $\nu=7/3$ is obtained, in both structures, when the $m=0$ branch of the 1LL is investigated). As a result, a collective Hall-like state is described with the fractional quantization of a transverse resistivity (just like for the ordinary FQHE state in the LLL), but the Laughlin correlations are described with a $q=1$ power in the Jastrow polynomial and loopless elements generate the system braid group (just like for the ordinary IQHE state in the LLL). We have, thus, stumbled across a novel phenomenon—the single-loop FQHE [51, 52]—which can be obtained only in higher Landau bands ($n>0$). We may also expect that this effect is very robust (simple, not structured, generators construction), which was confirmed in transport measurements of typical 2DEG structures and monolayer graphene samples [20, 40–42, 53].

In higher LLs it is possible that the cyclotron orbit surface is greater than the separation of neighboring particles (classical—as arguments of Ψ_N or M^N coordinates). Thus, for selected filling factors a single-loop path (as a representative of an element from the system braid group) can be generated as a double exchange of x-order neighbors (with integer x), $(\sigma_{i+1}\dots\sigma_{i+x-1}\dots\sigma_i^{-1}\sigma_{i+1}^{-1})^2$. This corresponds to the situation when exactly ϕ_0/x is attributed to a single electron from the partially filled level,

http://dx.doi.org/10.5772/64018

$$\begin{cases} \dfrac{N_0}{N-(2n+m)N_0}=\dfrac{2n+1}{x}\rightarrow \nu=2n+m+\dfrac{x}{2n+1} & \textit{for conventional} \\ \dfrac{N_0}{N-(4n-2+m)N_0}=\dfrac{2n+1}{x}\rightarrow \nu=4n-2+m+\dfrac{x}{2n+1} & \textit{for graphene} \end{cases} \tag{25}$$

Note that complete filling of the n'th LL is achieved when $x=2n+1$ and the braid group is generated by the loopless exchanges of particles and their $(2n+1)$-order neighbors.

2. In higher Landau bands also exists a possibility that the cyclotron orbit is too small to reach a neighboring (classical) carrier and, hence, the loopless exchanges are not allowed and need to be excluded from $\pi_1(\Omega)$. Fortunately, we can consider—similarly as in the LLL case—more structured, multi-loop exchanges to provide generators of the braid group describing the system. Commensurability conditions, which allow to establish the corresponding filling factors (connected with subgroups generated by b_i elements), resemble ones introduced for the zeroth Landau band. However, while possible ν for Hall-like states, we need to remember about a different number of flux quanta grasped by the cyclotron orbit ($(2n+1)\phi_0$ in the n'th LL). Additionally, we cannot take into account all particles in the system, but only those, which are placed in a partially filled level. Finally, we remind that if we consider a q-looped trajectory encircled in a 2D space, then all q loops must share the total magnetic field flux per particle, which is evidenced by a single-loop path.

To obtain a hierarchy—which resembles Jain's pyramid of fillings—we assume that $q-1$ loops experience exactly $(2n+1)\phi_0$ per particle, while the last one embraces a reduced portion, $(2n+1)\phi_0/x$, attributed to a single carrier. Thus, the appropriate commensurability conditions (with different, integer x) take the form of,

$$\begin{cases} \dfrac{N_0}{N-(2n+m)N_0}=(2n+1)\cdot(q-1)\pm(2n+1)\dfrac{1}{x} & \textit{for conventional} \\ \dfrac{N_0}{N-(4n-2+m)N_0}=(2n+1)\cdot(q-1)\pm(2n+1)\dfrac{1}{x} & \textit{for graphene} \end{cases} \tag{26}$$

with filling factors, which satisfy the requirements above, belonging to the set,

$$\begin{cases} \nu=2n+m+\dfrac{1}{(2n+1)\cdot\left[(q-1)\pm 1/x\right]} & \textit{for conventional} \\ \nu=4n-2+m+\dfrac{1}{(2n+1)\cdot\left[(q-1)\pm 1/x\right]} & \textit{for graphene} \end{cases} \tag{27}$$

Note that—despite the general similarity to the CF hierarchy—a supplementary factor, $2n+1$, is included in the denominators of all fractions from Eq. 27 (as a consequence of an enhanced kinetic energy). The last winding of a q-looped trajectory, for these fillings, fits perfectly to the area embraced by x classical particles. As a consequence, exchanges of x'th order neighbors are allowed and, thus, elements

$$b_i^{(q)} = \sigma_i^{q-1}\sigma_i\sigma_{i+1}\ldots\sigma_{i+x-1}^{\pm 1}\ldots\sigma_i^{-1}\sigma_{i+1}^{-1} \tag{28}$$

generate the cyclotron subgroup for the system.

3. Finally, the pairing of electrons—which occurs as a result of the Fermi sea instability—can also be investigated. In this case the number of particles is reduced by half and it is reasonable to consider the IQHE formation (for pairs),

$$\begin{cases} \dfrac{N_0}{N-(2n+m)N_0} = 2 \rightarrow \nu = 2n+m+\dfrac{1}{2} & \textit{for conventional} \\ \dfrac{N_0}{N-(4n-2+m)N_0} = 2 \rightarrow \nu = 4n-2+m+\dfrac{1}{2} & \textit{for graphene} \end{cases} \tag{29}$$

The equation above is constructed in such a manner that implementing a decreased number of particles— $\frac{N-(2n+m)N_0}{2}$ or $\frac{N-(4n-2+m)N_0}{2}$ —leads to the exact IQHE commensurability condition.

We have presented hierarchies that gather all filling factors (from all LLs) in which particles can experience quantum Hall effects in typical semiconductor and monolayer graphene samples. We have also explicitly presented these results, for the first Landau band, in **Tables 2** and **3**.

3.2. Bilayer graphene

The FQHE in bilayer systems (not only bilayer graphene) is exceptional, as noticed earlier by Eisenstein [54]. The unparalleled basic set of fillings – with $\nu=1/2$ being the most robust incompressible state – has its origin in the appearance of an additional surface [28, 55]. The supplementary sheet of carbon atoms, coupled to the primary one by a nonzero hopping integral [36–39], leads to the electron density located in both graphene planes. As a result, bilayer graphene samples are not strictly two-dimensional. Classically (trajectories, which represent elements of the system braid group, are classical), this means that particles can move freely between opposite layers of the structure. Thus, while considering whether the cyclotron orbit area is sufficiently large to enable the existence of particle exchanges in the system, graphene planes should not be investigated separately. For example, the $\nu=1$ state—corresponding to the integer phenomenon—is realized when the single-loop cyclotron path

http://dx.doi.org/10.5772/64018

encircles a surface equal to S/N, and not $2S/N$. However, while examining states described by fractional fillings of the LLL, even more interesting feature is revealed. Since multi-looped trajectories can be partly located in both graphene layers, the surface (and flux) provided by the additional plane needs to be taken into account. It is expected that the most energetically efficient trajectory is realized, when only one loop embraces (utilizes) the supplementary surface and magnetic field flux. As a consequence, its dimensions are not raised—they are equal to those of a single-loop path. Simultaneously, remaining loops ($q-1$ in the case of a q-looped trajectory) share the total per particle quantity, BS/N, associated with the primary layer. Latter results in a novel form of the commensurability conditions,

$$\frac{BS}{N} = \frac{1}{\nu}\phi_0 = (q-2)\phi_0 \pm \frac{1}{x}\phi_0 \tag{30}$$

with the hierarchy of fillings being a modified version of the composite fermion pyramid,

$$\nu = \left((q-2) \pm \frac{1}{x} \right)^{-1} \tag{31}$$

Here we have assumed that one of $q-2$ loops evidences a diminished (per particle) portion, $\pm\frac{1}{x}\phi_0$. Thus, it fits perfectly to the separation of an arbitrary particle and its x-order neighbors (as Ψ_N arguments) and allows them to exchange. Additionally, we speculate that the latter loop can be overwrapped in the direction opposite to one enforced by an external magnetic field (a minus sign in Eq. 31).

Even-denominator filling factors form a basic set—they are expected to be associated with most prominent Hall-like states [22–24] However, ratios with odd denominators are also included in the above hierarchy. The latter can be seen in **Table 4**, which gathers results from the whole LLL (and 1LL). In this paper we assumed that spin-valley branches of zeroth and first Landau bands, accessible for free electrons, are filled alternately. In other words, these sublevels are placed on the energy axis in the following order, $0K'\uparrow$, $1K'\uparrow$, $0K'\downarrow$, $1K'\downarrow$. Thus, filling factors responsible for the FQHE plateaus—n the $2<\nu<3$ range—are defined by the hierarchy from Eq. 33 (with a constant "+2" shift).

Although an even number of loops, $q-1$, is explicitly included in the commensurability conditions, it is an odd number, q, that constitutes a multi-looped trajectory (which represents a square of the cyclotron subgroup generator). This results in the Laughlin correlations with an odd power in the Jastrow-like polynomial—the multi-particle wave function is antisymmetric even for $\nu=1/2$ state.

In bilayer graphene, similarly as in typical 2DEG and monolayer graphene structures, kinetic energy of particles increases with Landau level index, n. Hence, the area encircled by a single-

loop cyclotron orbit (representing a braid group element) is also enhanced, $(2n+1)hc/eB$, and it embraces precisely $(2n+1)$ quanta of the magnetic field flux. This leads to commensurability conditions, which resemble ones already presented in this section and other authors' papers [10, 52, 55]. We investigate them very briefly,

Sublevel	Single-loop FQHE	Paired IQHE	q	ν	FQHE
$0K'\uparrow$			3	$\frac{1}{1+1/x}$	$\mathbf{\frac{1}{2}}, \mathbf{\frac{2}{3}}, \left(\mathbf{\frac{1}{3}}\right), \frac{3}{4}, \frac{4}{5}, \ldots$
			5	$\frac{1}{3-1/x}$	$\mathbf{\frac{1}{2}}, \mathbf{\frac{2}{5}}, \frac{3}{8}, \frac{4}{11}, \ldots$
			5	$\frac{1}{3+1/x}$	$\frac{1}{4}, \frac{2}{7}, \frac{3}{10}, \frac{4}{13}, \ldots$
$1K'\uparrow$	$\mathbf{\frac{4}{3}}, \mathbf{\frac{5}{3}}$	$\frac{3}{2}$	3	$1+\frac{1}{3\cdot(1-1/x)}$	$\mathbf{\frac{5}{3}}, \left(\mathbf{\frac{4}{3}}\right), \frac{3}{2}, \frac{13}{9}, \ldots$
			3	$1+\frac{1}{3\cdot(1+1/x)}$	$\frac{7}{6}, \frac{11}{9}, \frac{5}{4}, \frac{19}{15}, \ldots$
			3	$1+\frac{1}{3\cdot(1/2-1/x)}$	$\mathbf{\frac{4}{3}}, \frac{7}{5}, \frac{13}{9}, \ldots$
$0K'\downarrow$			3	$2+\frac{1}{1+1/x}$	$\mathbf{\frac{5}{2}}, \mathbf{\frac{8}{3}}, \frac{11}{4}, \frac{14}{5}, \ldots$
			5	$2+\frac{1}{3-1/x}$	$\mathbf{\frac{5}{2}}, \mathbf{\frac{12}{5}}, \frac{19}{8}, \frac{26}{11}, \ldots$
			5	$2+\frac{1}{3+1/x}$	$\frac{9}{4}, \frac{16}{7}, \frac{23}{10}, \frac{30}{13}, \ldots$
$1K'\downarrow$	$\mathbf{\frac{10}{3}}, \mathbf{\frac{11}{3}}$	$\frac{7}{2}$	3	$3+\frac{1}{3\cdot(1-1/x)}$	$\mathbf{\frac{11}{3}}, \left(\mathbf{\frac{10}{3}}\right), \frac{7}{2}, \frac{31}{9}, \ldots$
			3	$3+\frac{1}{3\cdot(1+1/x)}$	$\frac{19}{6}, \frac{29}{9}, \frac{13}{4}, \frac{49}{15}, \ldots$
			3	$3+\frac{1}{3\cdot(1/2-1/x)}$	$\mathbf{\frac{10}{3}}, \frac{17}{5}, \frac{31}{9}, \ldots$

Where q = the number of half loops in the exchange trajectory, ν = the hierarchy of fillings. Plus or minus signs denote the d irection of a last loop in the multi-loop cyclotron path. Selected hole states are indicated in brackets. Experimentally observable ratios are highlighted - a blue colour for ν possible to explain within the CF model and a red colour for ν out of the Jain hierarchy. Additionally, results for different sublevels are separated by three lines.

Table 4. LLL and 1LL filling factors obtained from the non-local theory (bilayer graphene).

http://dx.doi.org/10.5772/64018

1. First, it is possible that the system braid group is generated by loopless exchanges of x-order neighbors. This corresponds to the situation where exactly $(2n+1)/x$ flux quanta are attributed to a single particle,

$$\frac{N_0}{N-\varepsilon N_0}=\frac{2n+1}{x}\rightarrow \nu=\varepsilon+\frac{x}{2n+1} \tag{32}$$

where ε counts completely filled Landau sublevels and $x=1, 2, \ldots, 2n+1$. Note that the IQHE is realized in the system when x equals $2n+1$ and the single-loop cyclotron orbit fits perfectly to the separation of a particle and its $(2n+1)$-order neighbor. For other values of x electrons experience the so-called single-loop FQHE – the phenomenon allowed only in higher Landau bands ($n>0$).

2. The $(q-1)/2$-loop exchanges of x-order neighbors (as arguments of Ψ_N or M^N coordinates) can become generators of the system braid group (a cyclotron subgroup), when loopless ones are not accessible. This is achievable when q-looped path is arranged as follows: all $q-2$ loops experience precisely $(2n+1)\phi_0$ per particle, while the last loop evidences only a residual portion attributed to a single electron, $\frac{(2n+1)}{x}\phi_0$,

$$\frac{N_0}{N-\varepsilon N_0}=(2n+1)(q-2)\pm\frac{(2n+1)}{x}\rightarrow \nu=\varepsilon+\frac{1}{(2n+1)[q-2\pm 1/x]} \tag{33}$$

It should be emphasized that—in the above commensurability condition—we have not considered an additional per particle quantity, $\frac{BS}{N}$, supplied by the second layer of the structure. The latter can be performed because a remaining loop of the trajectory utilizes the supplementary magnetic field flux—it can be, thus, omitted in Eq. 33.

3. Finally, the pairing of electrons—which occurs as a result of the Fermi sea instability—can also be investigated. In this case the number of particles is reduced by half and it is reasonable to consider the IQHE formation (for pairs),

$$\frac{N_0}{N-\varepsilon N_0}=2\rightarrow \nu=\varepsilon+\frac{1}{2} \tag{34}$$

The above equation is constructed in such a manner that implementing a decreased number of particles, $\frac{N-\varepsilon N_0}{2}$, leads to the exact IQHE commensurability condition.

We have presented hierarchies that gather all filling factors (from all LLs) in which particles can experience quantum Hall effects. We have also explicitly presented these results—for lowest and first Landau bands—in **Table 4**.

A careful reader probably has already noticed that an application of the non-local theory of Hall systems to structures with a greater (than two) number of layers is straightforward. The most important modification concerns the commensurability conditions for q-looped cyclotron trajectories (when only multi-loop exchanges are accessible and generate the braid group describing the system). Each additional layer of atoms supplies an additional surface (and magnetic field flux) that needs to be embraced by this path. The most energetically efficient trajectory seems to be achieved when every added plane is utilized by a single loop. Dimensions of these loops are not raised and they are not included, at least explicitly, in the commensurability conditions. As a result, only remaining $q-\gamma$ ones (where γ stands for the number of supplementary layers) must share the total flux per particle, $BS/(N-\varepsilon N_0)$, which is experienced by the single-loop path.

4. Comparison between theory and experiment

As mentioned previously, scientists are currently unable to understand the entire physics behind the fractional quantum Hall effect. Experimenters constantly conduct novel analyses to gain an insight into this non-trivial phenomenon. As a result, many measuring techniques have been developed—the local compressibility measurements or experiments in Hall-bar and two-terminal geometries. Selected results, for all structures considered in this chapter, are presented in **Figure 1**. It is also worth emphasizing that experiments carried out in monolayer and bilayer graphene samples are exceptional. For example, it is possible to modify the carrier density (with a lateral gate voltage) in a fixed magnetic field strength (**Figure 1b** and **c**).

Figure 1a presents a very famous transport measurement conducted on a typical GaAs/AlGaAs quantum well sample (and published in the Pan et al. paper [19]). Its uniqueness is owed to the well-developed plateaus in the longitudinal resistance for LLL fillings which are impossible to obtain within the quasi-particle approach (at least without implementing residual and unclear interactions between CFs) [16, 17]. The appearance of these incompressible states can be, however, explained by the non-local theory of quantum Hall effects. Consider a multi-loop cyclotron trajectory of a particle (as M^N coordinate) that represents a square of the system braid group generator. It is probable that additional loops, belonging to this path, fit to the separation of higher order (not nearest) neighbors. In this case the incompressible Hall-like state can also be formed—which was confirmed by Pan's experiment—but it cannot be captured by Jain's model. The latter is owed to the fact that every flux quanta pinned to an electron is a convenient model of a supplementary loop in the cyclotron trajectory only when it fits perfectly to the inter-particle distance.

A surprising form of the basic set in bilayer graphene samples—where $\nu=1/2$ is the most prominent incompressible state—can be observed in transport measurements depicted in **Figure 1b**. We have already mentioned that this feature follows immediately from the necessity to embrace (by the multi-loop cyclotron path) a flux supplied by the additional layer (surface). One loop is, thus, wasted on the utilization and falls out from the commensurability conditions—the obtained hierarchy contains even-denominator filling factors. However, the exchange

http://dx.doi.org/10.5772/64018

trajectory (representing a braid group generator) consists of an odd number of half loops that protects the antisymmetric character of a particle statistics.

Finally, another interesting feature is worth to be noted—the remarkable stability of incompressible Hall-like states for $\nu = 7/3,\ 8/3$ and 5/2. The unexpected robustness of related plateaus makes "7/3 and 8/3 states unlikely to be the analogues of the 1/3, 2/3 Laughlin correlated states" [40]. This conclusion seems to agree with the non-local theory predictions. The braid group describing the system for these fillings (connected with the paired IQHE and the single-loop FQHE) is generated with loopless exchanges. Thus, the Laughlin correlations are described by a $p = 1$ power in the Jastrow polynomial, despite the fractional quantization of a transverse resistivity. Hence, the robustness of these states is expected to exceed one for the ordinary FQHE states, which was confirmed experimentally (**Figure 1c** and **d**).

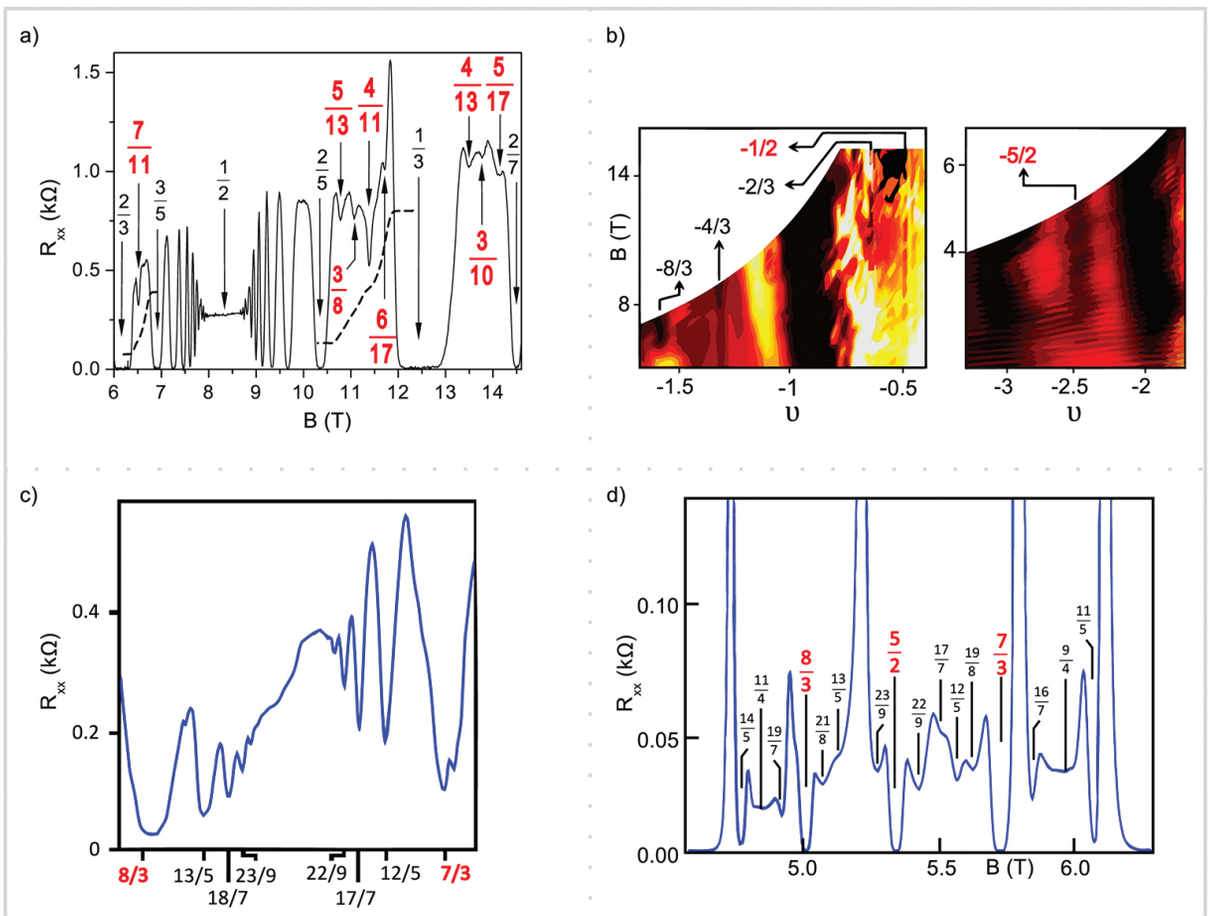

Figure 1. (a) Typical semiconductor quantum well. A longitudinal resistance as a function of external magnetic field. The figure is based on the Pan et al. paper [19]. (b) Bilayer graphene. A longitudinal resistance as a function of a magnetic field and a filling factor. $R_{xx} \approx 0.1[\Omega]$ is colored dark red and $R_{xx} \approx 4[k\Omega]$ is colored bright yellow. The figure is based on the Ki et al. paper [23]. (c) Monolayer graphene. A longitudinal resistance as a function of a filling factor. The figure is based on Amet et al.'s [53] paper. (d) Typical semiconductor quantum well. A longitudinal resistance as a function of external magnetic field. The figure is based on the Choi et al.'s [40] paper. Important filling factors (e.g. falling out of the CF hierarchy or corresponding to the single-loop FQHE) are highlighted.

5. Concluding remarks

In conclusion, the topological approach to quantum Hall effects is based on a concept of braid groups and their reduction stimulated by an external magnetic field (in 2D spaces). This model can be used to derive hierarchies of FQHE fillings for various two-dimensional structures (including multi-layers), which fit perfectly to the experimental findings. Additionally, it can be used to explain many issues that are believed to be mysterious—the puzzles of quantum Hall structures.

Acknowledgements

Support from the NCN Project UMO-2011/02/A/ST3/00116 is acknowledged.

Author details

Patrycja Łydżba* and Janusz Jacak

*Address all correspondence to: patrycja.lydzba@pwr.edu.pl

Faculty of Fundamental Problems of Technology, Wroclaw University of Science and Technology, Wrocław, Poland

References

[1] Boebinger GS, Chang AM, Stormer HL, Tsui DC. Magnetic field dependence of activation energies. Physical Review Letters. 1985; 55(15):1606–1609.

[2] Tsui DC, Stormer HL, Gosard AC. Two-dimensional magnetotransport in the extreme quantum limit. Physical Review Letters. 1982; 48(22):1559–1562.

[3] Bonsall L, Maradudin AA. Some static and dynamical properties of a two-dimensional Wigner crystal. Physical Review B. 1977; 15(4):1959–1973.

[4] Laughlin RB. Anomalous quantum hall effect: an incompressible quantum fluid with fractionally charged excitations. Physical Review Letters. 1983; 50(18):1395–1398.

[5] Aharonov Y, Bohm D. Significance of electromagnetic potentials in the quantum theory. The Physical Review. 1959; 115(3):485–491.

[6] Berry MV. Classical adiabatic angles and quantal adiabatic phase. Journal of Physics A: Mathematical and General. 1985; 18:15–27.

[7] Arovas D, Schrieffer JR, Wilczek F. Fractional statistics and the quantum Hall Effect. Physical Review Letters. 1984; 53(7):722–723.

[8] Read N. Theory of the half-filled Landau level. Semiconductor Science and Technology. 1994; 9:1859–1864.

[9] Jacak J, Jóźwiak I, Jacak L. New implementation of composite fermions in terms of subgroups of a braid group. Physics Letters A. 2009; 374:346–350.

[10] Jacak J, Łydżba P, Jacak L. Fractional quantum Hall effect revisited. Physica B. 2015; 475:122–139.

[11] Jacak J, Łydżba P, Jacak L. Homotopy approach to fractional quantum Hall Effect. Applied Mathematics. 2015; 6:345–358.

[12] Jain JK, Kamilla RK. Quantitative study of large composite-fermion systems. Physical Review B. 1997; 55(8):417–420.

[13] Girvin M. Introduction to the fractional quantum Hall effect. Seminaire Poincare. 2004; 2:53–74.

[14] Chakraborty T, Pietilainen P. The fractional quantum Hall effect, properties of an incompressible quantum fluid. Springer-Verlag, Berlin-Heidelberg-New York-London-Paris-Tokyo; 1988 .

[15] Haldane FDM. Fractional quantization of the Hall effect: a hierarchy of incompressible quantum fluid states. Physical Review Letters. 1983;51(7):605–608.

[16] Jain JK. Composite-fermion approach for the fractional quantum Hall effect. Physical Review Letters. 1989; 63:199–202.

[17] Jain JK. A note contrasting two microscopic theories of the fractional quantum Hall effect. Indian Journal of Physics. 2014; 88:915–929.

[18] Landau LD. The theory of a Fermi liquid. Soviet Physics JETP. 1957; 3(6):920–925.

[19] Pan W et al. Fractional quantum Hall effect of composite fermions. Physical Review Letters. 2003; 90(1):016801.

[20] Pan W et al. Experimental studies of the fractional quantum Hall effect in the first excited Landau level. Physical Review Letters. 2003; 90:075307.

[21] Mandal SS and Jain JK. Theoretical search for the nested quantum Hall effect of composite fermions. Physical Review B. 2002; 66:155302.

[22] Kou A et al. Electron-hole asymmetric integer and fractional quantum Hall effect in bilayer graphene. Science. 2014; 345(6192):55–57.

[23] Ki D, Fal'ko VL, Abanin DA, Morpurgo AF. Observation of even denominator fractional quantum Hall effect in suspended bilayer graphene. Nano Letters. 2014; 14:2135–2139.

[24] Bao W et al. Magnetoconductance oscillations and evidence for fractional quantum Hall states in suspended bilayer and trilayer graphene. Physical Review Letters. 2010; 105:246601.

[25] Birman JS. Braids, links, and mapping class groups. Princeton University Press. 1975; (No. 82).

[26] Sudarshan ECG, Imbo TD, Imbo CS. Topological and algebraic aspects of quantization: symmetries and statistics. Annales de l'Institut Henri Poincaré, Section A. 1988; 49(3): 387–396.

[27] MacKenzie R. Path integral methods and applications. arXiv:quant-ph/0004090. 2000 .

[28] Łydżba P, Jacak J. Topological origin of all incompressible states from the lowest Landau level: Preliminary results on wave functions. Forthcoming.

[29] Wexler C, Ciftja O. Novel liquid crystalline phases in quantum Hall systems. International Journal of Modern Physics B. 2006; 20(7):747–778.

[30] Williams FIB. Experiments on melting in classical and quantum two dimensional electron systems. In: International Conference on Physics in Two Dimensions, 1991. Helvetica Physica Acta, Switzerland; 1992.

[31] Du X et al. Fractional quantum Hall effect and insulating phase of Dirac electrons in graphene. Nature. 2009; 462:192–195.

[32] Pan W et al. Fractional quantum Hall effect at Landau level filling ν=4/11. Physical Review B. 2015; 91:041301.

[33] Samkharadze N et al. Observation of incompressibility at ν=4/11 and ν=5/13. Physical Review B. 2014; 91:081109.

[34] Stormer HL. Nobel lecture: the fractional quantum Hall effect. Reviews of Modern Physics. 1999; 71(4):875–889.

[35] Du RR et al. Experimental evidence for new particles in the fractional quantum Hall effect. Physical Review Letters. 1993; 70(19):2944–2947.

[36] Goerbig MO. Electronic properties of graphene in a strong magnetic field. Reviews of Modern Physics. 2011; 83:1193–1243.

[37] McCann E. Electronic properties of monolayer and bilayer graphene. NanoScience and Technology. 2012; 57:237–275. DOI: 10.1007/978-3-642-22984-8_8.

[38] Novoselov KS. Unconventional quantum Hall effect and Berry's phase of 2π in bilayer graphene. Nature Physics. 2006; 2:177–180.

[39] Fal'ko VL. Electronic properties and the quantum Hall effect in bilayer graphene. Philosophical Transactions of the Royal Society A. 2008; 366:205–219.

[40] Choi HC et al. Activation gaps of fractional quantum Hall effect in the second Landau level. Physical Review B. 2008; 77:081301.

[41] Dean CR et al. Contrasting behavior of the 5/2 and 7/2 fractional quantum Hall effect in a tilted field. Physical Review Letters. 2008; 101:186806.

[42] Eisenstein JP. New physics in high Landau levels. Physica E: Low-dimensional Systems and Nanostructures. 1999; 6: 29–35.

[43] Lee DS et al. Transconductance fluctuations as a probe for interaction-induced quantum Hall states in graphene. Physical Review Letters. 2012; 109:056602.

[44] Bolotin KI. Observation of the fractional quantum Hall effect in graphene. Nature Letters. 2009; 462:196–199.

[45] Skachko I. Fractional quantum Hall effect in suspended graphene probed with two-terminal measurements. Philosophical Transactions of the Royal Society A. 2010; 368:5403–5416.

[46] Feldman BE. Fractional quantum Hall phase transitions and four-flux states in graphene. Physical Review Letters. 2013; 111:076802.

[47] Feldman BE. Unconventional sequence of fractional quantum Hall states in suspended graphene. Science Reports. 2012; 337:1196–1199.

[48] Ghahari F. Measurement of the v=1/3 fractional quantum Hall energy gap in suspended graphene. Physical Review Letters. 2011; 106:046801.

[49] Peterson MR, Nayak C. Effects of Landau level mixing on the fractional quantum Hall effect in monolayer graphene. Physical Review Letters. 2014; 113:086401.

[50] Dean CR. Multicomponent fractional quantum Hall effect in graphene. Nature Physics. 2011; 7:693–696.

[51] Łydżba P, Jacak L, Jacak J. Hierarchy of fillings for the FQHE in monolayer graphene. Scientific Reports. 2015; 5:1–16.

[52] Jacak J, Jacak L. The commensurability condition and fractional quantum Hall effect hierarchy in higher Landau levels. Pisma v ZhETF. 2015; 102:19–25.

[53] Amet F et al. Composite fermions and broken symmetries in graphene. Nature Communications. 2015; 6:1–7.

[54] Eisenstein JP. New fractional quantum Hall state in double-layer two-dimensional electron systems. Physical Review Letters. 1992; 68(9):1383–1386.

[55] Jacak J, Jacak L. Difference in hierarchy of FQHE between monolayer and bilayer graphene. Physical Letters A. 2015; 379:2130–2134.

IntechOpen